



Original Article

Identification and functional characterization of a new flavonoid glycosyltransferase from *Rheum palmatum*

Shiwen Zhang^a, Jianzhen Zou^a, Zitong Hao^a, Mengqi Gao^a, Gang Zhang^{b,*}, Mengmeng Liu^{a,*}

^a College of Traditional Chinese Medicine, Hebei University, Baoding 071002, China

^b Shaanxi Qinling Application Development and Engineering Center of Chinese Herbal Medicine, College of Pharmacy, Shaanxi University of Chinese Medicine, Xi'an 712046, China

ARTICLE INFO

Article history:

Received 18 April 2024

Revised 12 June 2024

Accepted 20 August 2024

Available online 22 August 2024

Keywords:

flavonoid
glycosyltransferase
homology modeling
molecular docking
Rheum palmatum L.
site-directed mutagenesis

ABSTRACT

Objective: To characterize a glycosyltransferase (RpUGT1) from *Rheum palmatum* and investigate its specificity toward flavonoid compounds.

Methods: The RpUGT1 was expressed in *Escherichia coli* and screened for catalytic activity against a range of flavonoid substrates using a high-throughput HPLC assay method. Mass spectrometry (MS) and nuclear magnetic resonance (NMR) were used to determine the structure of the product. Homology modeling, molecular docking analyses and site-directed mutagenesis studies were conducted to identify key residues responsible for its function.

Results: The recombinant RpUGT1 protein exhibited catalytic activity towards various flavonoids. Notably, RpUGT1 catalyzed the glycosylation of isorhamnetin to form 3-O-glucoside and kaempferol to form 7-O-glucoside, utilizing uridine diphosphate (UDP) glucose as the sugar donor. The homology modeling and molecular docking analyses identified key residues responsible for its activity. Subsequent site-directed mutagenesis studies highlighted the crucial role of K307 in catalysis.

Conclusion: These discoveries offer valuable perspectives on the role of the UGT family and establish a groundwork for forthcoming research on the synthesis of flavonoids in plants.

© 2024 Tianjin Press of Chinese Herbal Medicines. Published by ELSEVIER B.V. This is an open access article under the CC BY-NC-ND license (<http://creativecommons.org/licenses/by-nc-nd/4.0/>).

1. Introduction

Flavonoids are widely distributed in various plant species and have a characteristic C6–C3–C6 backbone (Cappello et al., 2016). Based on their oxidation status and substitution patterns, flavonoids can be categorized into various subgroups, which encompass flavanones, dihydroflavonols, flavones, flavonols, flavan-3,4-diols, flavan-3-ols, and anthocyanins (Wang et al., 2023). These compounds possess significant medicinal properties, such as antiviral activity, antioxidant, antibacterial, and anti-inflammatory activities (Mossa et al., 2015, Kumar, Singla, Dandriyal, & Jaitak, 2018, Xu, Chen, Zhang, & Liang, 2021), and their structural diversity can be further enhanced through modifications like glycosylation, acylation, and methylation, which can further enhance their structural diversity (Vasudevan & Lee, 2020).

Glycosylation is a prevalent structural modification found in secondary natural products, contributing to the stability, solubility, and diversity of aglycons (Li, Baldauf, Lim, & Bowles, 2001, Pei et al., 2022, Xu et al., 2022). In plants, uridine diphosphate (UDP)-dependent glycosyltransferases (UGTs) are responsible for

catalyzing these reactions. UGTs transfer monosaccharide moieties from activated nucleotide sugars to acceptor molecules, including carbohydrates, glycosides, oligosaccharides, and polysaccharides.

Recent years have witnessed the functional characterization of numerous flavonoid glycosyltransferases from various plant species, such as *Glycyrrhiza uralensis* Fisch., *Vitis vinifera* L., *Malus pumila* M. and *Camellia sinensis* (L.) Kuntze (Ono et al., 2010, Dai et al., 2017, Chen et al., 2019, Xie et al., 2020). Many of these enzymes exhibit high catalytic activity toward flavones and flavonols, leading to the formation of their respective 7-O-glycosides or 3-O-glycosides. *Rheum palmatum* L., a valuable traditional medicinal herb, contains diverse anthraquinones, including rhein, emodin, chrysophanol, and physcion (Zhai et al., 2023). These anthraquinones have garnered significant research and commercial attention due to their wide range of bioactivities, such as antibacterial, antioxidant, anti-malarial, and antitumor properties (Koumaglo, Gbeassor, Nikabu, de Souza, & Werner, 1992, Sittie et al., 1999, Akhtar et al., 2013, Sun et al., 2019). While key genes involved in the biosynthetic pathways of anthraquinones have been identified and characterized (Huo, Zhang, & Liu, 2020), the flavonoid glycosyltransferases in *R. palmatum* have not been fully investigated.

This study presents the discovery of a novel glycosyltransferase, RpUGT1, from *R. palmatum*. Through heterologous expression and functional characterization, it was demonstrated that recombinant

* Corresponding authors.

E-mail addresses: jay_gumling2003@aliyun.com (G. Zhang), mmliu1987@outlook.com (M. Liu).

RpUGT1 can catalyze the glucosylation of kaempferol and isorhamnetin, with regioselectivity occurring at the 7-OH position of kaempferol and the 3-OH position of isorhamnetin. Furthermore, the catalytic characteristics of RpUGT1, along with the essential residues contributing to its catalytic ability, were assessed through techniques such as homology modeling, AutoDock analysis, and site-directed mutagenesis.

2. Materials and methods

2.1. Plant materials and chemicals

Specimens (HBU071001) of *R. palmatum* were collected from the Hezheng, Gansu Province, and identified by Professor Gang Zhang from Shaanxi University of Chinese Medicine.

Kaempferol (Lot: AFBL0751, MW: 286.23), isorhamnetin (Lot: AFBL0623, MW: 316.26), quercetin (Lot: AFBL2146, MW: 302.24), luteolin (Lot: AFBL3018, MW: 286.24), apigenin (Lot: AFBL4016, MW: 270.24), diosmetin (Lot: AFBL0985, MW: 300.26), baicalein (Lot: AFBL4267, MW: 270.24), phloretin (Lot: AFBL2146, MW: 274.27), naringenin (Lot: AFBL5327 MW: 272.25), daidzein (Lot: AFBL8691, MW: 254.24), UDP-glucose (Lot: AFBL521875, MW: 566.30), chromatographic methanol (Lot: AFBL631963, MW: 32.04) and formic acid (Lot: AFBL221456, MW:46.03) were purchased from Chengdu Alfa Biotechnology Co., Ltd. (Chengdu, China).

2.2. Molecular cloning of RpUGT1 from *R. Palmatum*

To obtain the full-length cDNA of RpUGT1, total RNA from *R. palmatum* leaves was isolated using the EASYspin Plus Plant RNA Kit (Beijing, China). The RNA extracted was then subjected to reverse transcription using the PrimeScript™ RT Reagent Kit (TaKaRa, Dalian, China) following the manufacturer's instructions, resulting in cDNA synthesis. For PCR amplification, gene-specific primer pairs and KOD One™ PCR Master Mix-Blue (TOYOBO, Japan) were employed. The PCR conditions were meticulously executed in accordance with the methodology employed in our previous study (Huo, Zhang, & Liu, 2020). Subsequently, the PCR product was purified and ligated into the pTOPO-TA/Blunt vector (Aidlab, Beijing, China). It was then transformed into *E. coli* Top10 for subsequent sequencing analysis.

2.3. Sequence alignment and phylogenetic analysis

We utilized the Bioedit 7.2 software package to perform sequence alignment between RpUGT1 and previously reported glycosyltransferases. We utilized a conserved domain instrument accessible at <https://www.ncbi.nlm.nih.gov/Structure/cdd/wrpsb.cgi> to analyze motifs and domains. To construct the phylogenetic tree, we utilized the neighbor-joining method with 1 000 bootstrap replicates in MEGA7 software (Kumar, Stecher, & Tamura, 2016). ClustalW was used to align the translated protein sequence of RpUGT1 with known plant glycosyltransferases obtained from the NCBI GenBank database.

2.4. Expression and purification of RpUGT1 protein

To produce the recombinant protein RpUGT1 in *E. coli* BL21(DE3) strain obtained from Takara (Dalian, China), subcloning of the coding regions into the expression vector HIS-MBP-pDB was performed. This subcloning procedure was carried out using the Seamless Cloning kit provided by Aidlab Biotech (Beijing, China). The vector, previously stored in our lab, was digested with EcoRI and XhoI restriction enzymes. A comprehensive list of primers employed in the process of vector construction was shown in Table S1. The PCR reaction conditions are the same as those used in our previous experiment (Huo,

Zhang, & Liu, 2020). After confirming the sequences, we conducted heterologous protein expression and purification following the same methods as in our previous study (Huo, Zhang, & Liu, 2020). Finally, the purified protein was stored at -80°C to preserve its catalytic activity for future assays.

2.5. Enzymatic activity assay of RpUGT1

To assess the catalytic capability of RpUGT1 *in vitro*, the following experimental procedure was employed. The enzyme reaction was conducted using a 100 mmol/L KH_2PO_4 - K_2HPO_4 buffer solution at pH 7.5. The reaction mixture consisted of 50 μg of recombinant RpUGT1 enzyme, 0.8 mmol/L UDP-glucose as the donor substrate, and 0.4 mmol/L specific substrate, with a total volume of 150 μL . Control assays were carried out without the inclusion of recombinant proteins.

The reactions were allowed to proceed at a temperature of 30°C for a duration of 12 h. To stop the reactions, 150 μL of methanol was added. The resulting reaction mixture was directly utilized for subsequent analysis using techniques such as high-performance liquid chromatography (HPLC), mass spectrometry (MS), and nuclear magnetic resonance (NMR). Control experiments were also conducted in the absence of recombinant proteins for comparison and reference purposes.

2.6. Effects of reaction time, pH value and temperature on enzyme activity and kinetic studies of RpUGT1

Several experiments were conducted to determine the optimal pH and reaction temperature for enzyme activity. To optimize the pH, 100 mmol/L buffers with different pH values were used, including citric acid-sodium citrate buffers ranging from pH 4.0 to 6.0, KH_2PO_4 - K_2HPO_4 buffers with a pH range of 7.0 to 8.0, a KH_2PO_4 - K_2HPO_4 buffer at pH 7.5, and Na_2CO_3 - NaHCO_3 buffers ranging from pH 9.0 to 10.0. For temperature optimization, the reactions were carried out at temperatures ranging from 10°C to 50°C , and the progress of the reaction was evaluated at various time points over a period of 0 to 24 h. The reaction mixture obtained from these experiments was directly analyzed using HPLC.

2.7. Molecular docking

The three-dimensional structure of RpUGT1 was predicted using Alphafold2, while the sequence alignment of RpUGT1 was obtained from the TM-align server. The root mean square deviation (RMSD) values were computed to evaluate the structural similarity of the predicted models, while the quality of the protein models was assessed through Verify-3D on the SAVES server.

Chemical formulas of small molecules, namely kaempferol, isorhamnetin, quercetin, luteolin, apigenin, diosmetin, baicalein, phloretin, naringenin daidzein, and UDP-glucose were generated using KingDraw. To investigate their binding interactions, docking studies were conducted using Autodock. The goal was to explore different conformations and orientations of the ligands within the catalytic site. Prior to docking, both the protein and ligand structures were prepared accordingly. The docking procedure employed protein-fixed ligand-flexible docking with the Lamarckian genetic algorithm (LGA) method. The conformation with the lowest binding energy was identified as the best candidate. To gain insight into the interactions between the protein and small molecules, PyMol was used for analysis purposes.

2.8. Mutagenesis of RpUGT1

For mutagenesis investigations, the wild-type gene of RpUGT1 was used as a reference. Site-directed mutagenesis was performed

using the Mut Express MultiS Fast Mutagenesis Kit. The mutants were generated by amplifying the optimized gene template, which was present in the HIS-MBP-pDB vector. The PCR-amplified mutant constructs were subsequently verified through PCR and sequencing to ensure the successful incorporation of the desired mutations. After confirmation, the mutant constructs were transformed into *E. coli* BL21(DE3) for heterologous expression, enabling the production of the mutated protein.

2.9. HPLC analysis

For the HPLC analysis, an Agilent 1260 Infinity HPLC system (Santa Clara, USA) was utilized. The system was equipped with a Dr. Maisch Repro Sil-Pur Basic-C₁₈ column (250 mm × 4.6 mm, 5 μm). The flow rate was set at 1 mL/min, and the column temperature was maintained at 30 °C. The detection of flavonol glycosides was performed at a specific wavelength of 346 nm. The separation employed a gradient elution method using water (0.1% formic acid) (A) and methanol (B). The gradient elution profile was as follows: starting with 35% B, increasing to 65% B over 0 to 20.0 min, further increasing to 100% B from 20.0 to 25.0 mins, and finally returning to 35% B from 25.0 to 30.0 min. The injection volume for each sample was 10 μL.

3. Results

3.1. Sequence analysis of RpUGT1

RpUGT1 has an open reading frame (ORF) length of 1 404 bp, which corresponds to the encoding of a protein comprising 484 amino acid residues (MT834516). The molecular weight of RpUGT1

was predicted to be 5.169×10^4 , and its isoelectric point was 5.81. The protein has a non-transmembrane nature, lacks a signal peptide, and is hydrophobic with a GRAVY (grand average of hydrophobicity) value of 0.005. The protein's aliphatic index was 91.78, and its instability index was 50.41. Subcellular localization analysis suggests that RpUGT1 was a cell membrane/chloroplast protein. The protein contains a conserved domain with a glycosyltransferase signature, indicating its potential as a UDP-glycosyltransferase (Fig. S1).

Based on the secondary structure prediction (Fig. S2), RpUGT1 exhibited an α -helical region, which encompassed approximately 41.97% of the protein. This α -helical segment was predominantly located in the N-terminal region. The protein also contained a random coil region, comprising approximately 37.26% of the protein, which was distributed throughout the chain. Furthermore, the extended chain region represented 14.78% of the protein, while the beta turn region accounted for 6.0% of the protein.

3.2. Phylogenetic analysis of RpUGT1

A neighbor-joining phylogenetic tree was generated using the MEGA7 software (Kumar, Singla, Dandriyal, & Jaitak, 2018) to analyze the relationship between RpUGT1 and other known CGTs and UGTs. The tree revealed that RpUGT1 clusters closely with *Fagopyrum esculentum* Moench, which is a congeneric species (Fig. 1).

3.3. Characterization of recombinant protein

The RpUGT1 gene was successfully inserted into the HIS-MBP-pDB expression vector successfully, resulting in the amplification

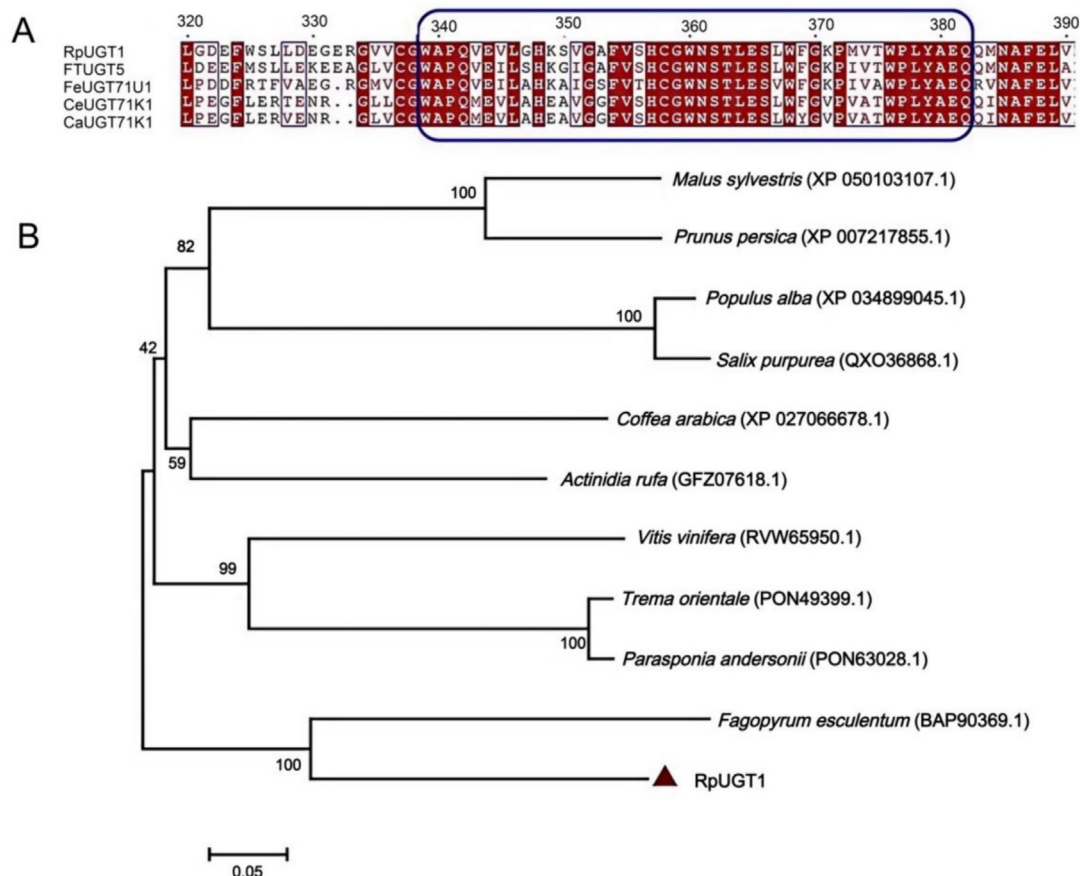


Fig. 1. Sequence alignment and phylogenetic analysis of UGT proteins. (A) Sequence alignment: Homologous UGTs from four plant species, including *Fagopyrum tataricum*, *F. esculentum*, *Coffea eugenioides* and *C. Arabica*. (B) Phylogenetic analysis of amino acid sequences of UGTs from various organisms was constructed using neighbor-joining method in MEGA 7, with 1 000 bootstrap replicates (condensed tree value $\geq 50\%$).

of a DNA fragment of around 2 000 bp (Fig. 2A). The recombinant RpUGT1 protein, which featured an N-terminal His-tag, was expressed in *E. coli* BL21(DE3) and exhibited a molecular weight of approximately 94 kDa, as detected through SDS-PAGE analysis. Purification of the recombinant protein was accomplished using Ni-NTA chromatography, and the presence of the desired protein was confirmed via SDS-PAGE analysis (Fig. 2B).

3.4. Substrate specificity of RpUGT1

To assess the glycosylation activity of RpUGT1, enzymatic assays were conducted using uridine diphosphate glucose (UDPG) as the sugar donor and ten flavonoid compounds as sugar acceptors. Among the tested compounds, only kaempferol and isorhamnetin were recognized by RpUGT1 and were catalyzed to form glycosylated products with higher polarity (Fig. 3). The formation of monoglucoside products was confirmed by conducting FTMS +p ESI-MS analysis. The analysis revealed ion peaks corresponding to the products, which exhibited a mass increase of 162 atomic mass units compared to the substrates. Based on NMR results, these structures were identified as kaempferol-7-O-glucoside and isorhamnetin-3-O-glucoside (Table S2 and S3).

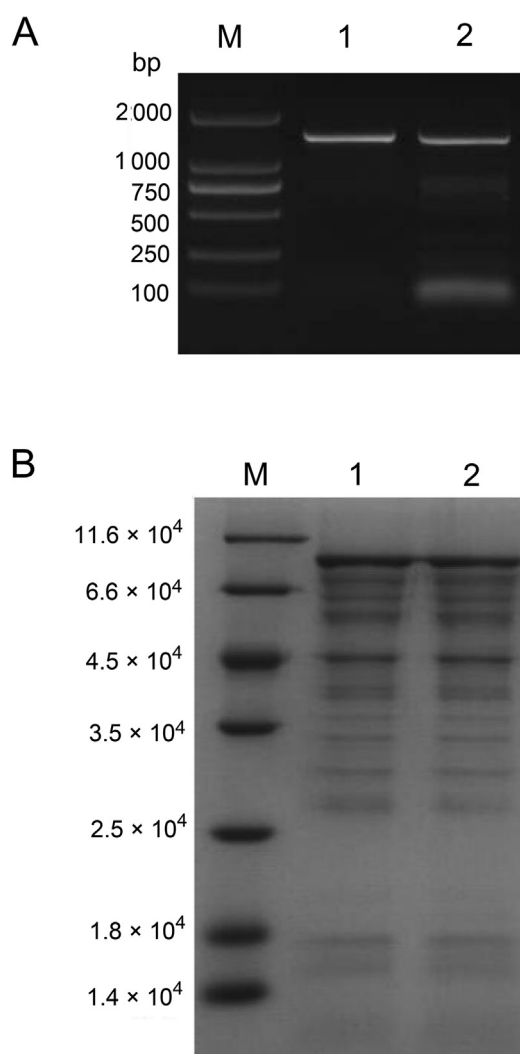


Fig. 2. Expression and purification of recombinant RpUGT1 protein. (A) PCR amplification and cloning of *RpUGT1* gene. M: marker; lane 1–4: PCR amplified *RpUGT1* gene. (B) Purified protein of RpUGT1 by SDS-PAGE. Lane M: markers; lane 1–2: HIS-MBP-pDB-RpUGT1.

3.5. Biochemical characterization and kinetic properties of RpUGT1

The biochemical properties of RpUGT1 were examined using kaempferol and isorhamnetin as sugar acceptors, and UDPG as the sugar donor. The catalytic activity of RpUGT1 was assessed across a temperature range of 10 to 50 °C, with optimal activity observed at 35 °C (Fig. 4A). Analysis of enzyme activity at various pH values (ranging from 4.0 to 10.0) revealed that the optimal pH for RpUGT1 was pH 7.5, using a 100 mmol/L KH_2PO_4 - K_2HPO_4 buffer (Fig. 4B). The yield of the glycosylated product exhibited a linear increase during the first hour, with the growth rate leveling off after 6 h (Fig. 4C).

The apparent K_m (Michaelis constant) value of RpUGT1 for kaempferol was determined to be $(517.9 \pm 7.2) \mu\text{mol/L}$, with a V_{max} of $(64.15 \pm 0.87) \text{mmol/L} \cdot \mu\text{g} \cdot \text{min}$. For isorhamnetin, the apparent K_m value of RpUGT1 was $(662.7 \pm 6.1) \mu\text{mol/L}$, with a V_{max} of $(68.50 \pm 0.37) \text{mmol/L} \cdot \mu\text{g} \cdot \text{min}$ (Table 1). The catalytic efficiency of RpUGT1 towards kaempferol was found to be higher than that towards isorhamnetin.

3.6. Homology modeling of RpUGT1 protein

The protein structures of RpUGT1 were predicted using AlphaFold2, a deep learning-based structure prediction method. Five models were generated, and the AlphaFold2-predicted structure obtained had an LDDT value of 89.175, indicating a high-quality prediction (Fig. 5A). To assess the quality of the top-ranked structure, Verify-3D analysis was performed using the SAVES server. A qualified model was defined as having over 80% of residues with a 3D/1D value greater than 0.1 and an insignificant fraction less than 0.1 (Fig. 5B). The results confirmed that the rank_1 protein structure is of sufficient quality to be utilized in molecular docking research.

3.7. Molecular docking and site-directed mutagenesis of residues in RpUGT1 protein

In order to enhance a deeper information of the active pocket of RpUGT1, molecular docking was conducted using UDPG as the sugar donor and kaempferol as the sugar acceptor. The binding sites of the glycosyl donor and acceptor were calculated and docked separately, as depicted in Fig. 6. The findings demonstrated that both binding pockets are situated within the deep cleft of the interaction area, tightly enclosed by the N-terminus and C-terminus domains of RpUGT1, and are spatially proximal to each other.

Similar to other plant UGTs, the C-terminus of RpUGT1 exhibits prominent interactions with the glycosyl donor. Furthermore, the surrounding residues in this region are highly conserved and predominantly hydrophilic. In particular, the residue S379 in this motif has the potential to form hydrogen bonds with the diphosphate group of UDPG. Our docking results also suggest that the residues H357, W360, and N361 may interact with the uridine group of UDPG, forming hydrogen bonds that contribute to the stabilization of the donor molecule within the active pocket.

To validate the functional importance of the predicted vital residues, we conducted alanine scanning mutagenesis on a total of eight selected sites. The catalytic activity of the resulting mutants was assessed using kaempferol as the substrate. HPLC analyses were performed to evaluate the glycosylation activity of these mutants. The results showed that when residues C134, W360, N361, Y379, H357, G15, K307, and S270 were mutated to alanine, the glycosylation activity of the protein was completely abolished for all detected molecules. The findings strongly suggest that these eight residues play critical roles in binding the UDPG donor and are essential for the glycosylation activity of RpUGT1.

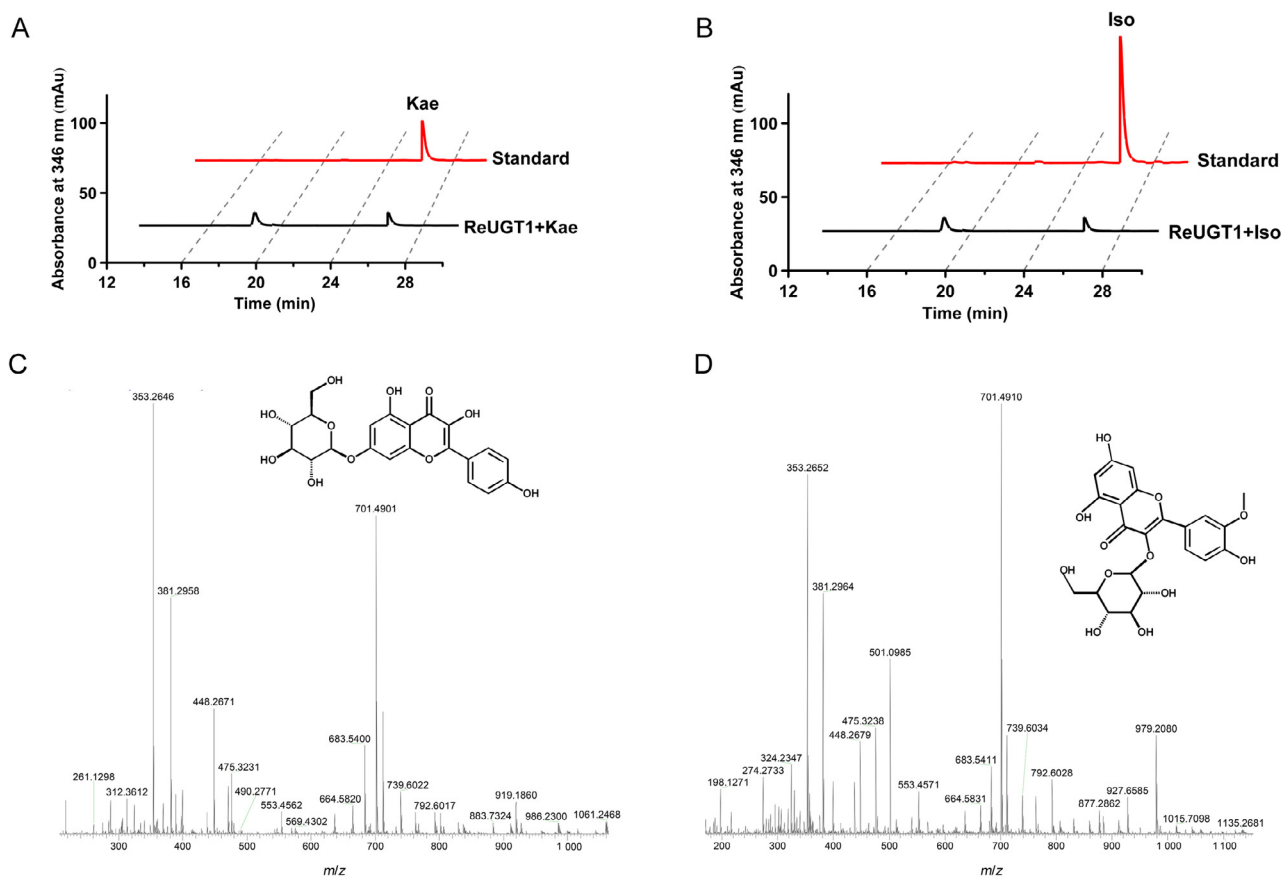


Fig. 3. RpUGT1 glycosylation reaction followed by HPLC and MS detection (Kae: kaempferol; Iso: isorhamnetin). HPLC analysis and catalytic reaction of RpUGT1 with kaempferol (A) and isorhamnetin (B) as substrates. MS detection of glycosylation products with kaempferol (C) and isorhamnetin (D) as substrates.

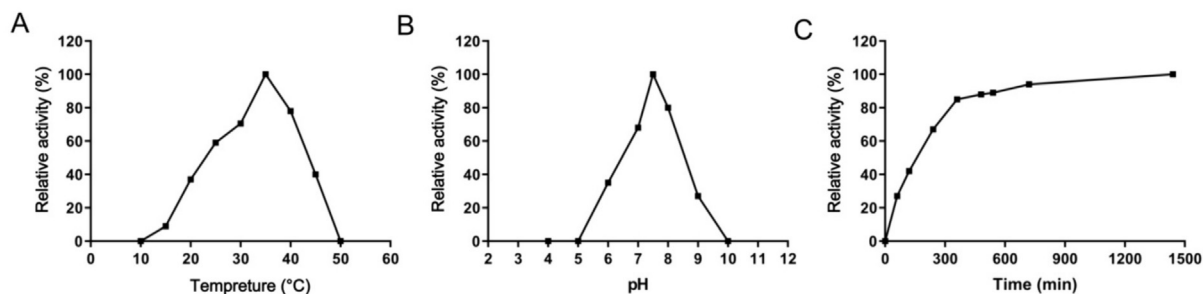


Fig. 4. Effects of reaction temperatures (A), buffer pH values (B) and reaction time (C) on activities of RpUGT1.

Molecular docking analyses were conducted on kaempferol to confirm the critical residues in the UDPG acceptor active pocket. Two salt bridges were observed between H16 and the hydroxyl (OH) group of kaempferol at positions C-3 (−3.5 Å) (1 Å = 0.1 nm) and C-4 (−3.2 Å), respectively (Fig. 6A). Additionally, a salt bridge was observed between K307 and the OH group of kaempferol at position C-7 (−3.0 Å). Notably, K307 is in close proximity to the 7-OH group, facilitating the deprotonation of the hydroxyl group at the C-7 position by K307, leading to the formation of a nucleophilic oxyanion. This oxyanion can subsequently attack the C1' carbon of UDPG, initiating the glycosylation reaction. The finding helps to explain why glycosylation primarily occurs at the 7-OH position of kaempferol. Furthermore, K307 is located at the cleft between the two binding sites and connects with both kaempferol and UDPG (Fig. 6B). Mutation of K307 to alanine results in the

total loss of enzyme activity, confirming its indispensable role as a crucial catalytic residue while stabilizing the UDPG donor.

4. Discussion

Glycosylation plays a vital role in the biosynthesis of secondary metabolites, enhancing the water solubility and reducing toxicity. Flavonoids, which are polyphenolic compounds found in plants, have garnered interest from researchers in medicinal chemistry and drug design due to their diverse biological and pharmacological properties (Khan et al., 2018). Both natural and synthetic flavonoids have been investigated for their potential health benefits. Glycosylation offers a means to expand the structural variety of flavonoids, enhance their solubility, and improve their bioavailability.

Table 1
Kinetic parameters of recombinant RpUGT1 using kaempferol and isorhamnetin as substrates and UDP-glucose as donor substrate.

Substrates	K_m ($\mu\text{mol/L}$)	V_{max} ($\text{mmol/L}\cdot\mu\text{g}\cdot\text{min}$)	k_{cat} ($\times 10^{-3}\cdot\text{S}^{-1}$)	k_{cat}/K_m ($\text{L/mol}\cdot\text{S}$)
Kaempferol	517.9 ± 7.2	64.15 ± 0.87	5.38 ± 0.42	10.39
Isorhamnetin	662.7 ± 6.1	68.50 ± 0.37	5.20 ± 0.35	7.85

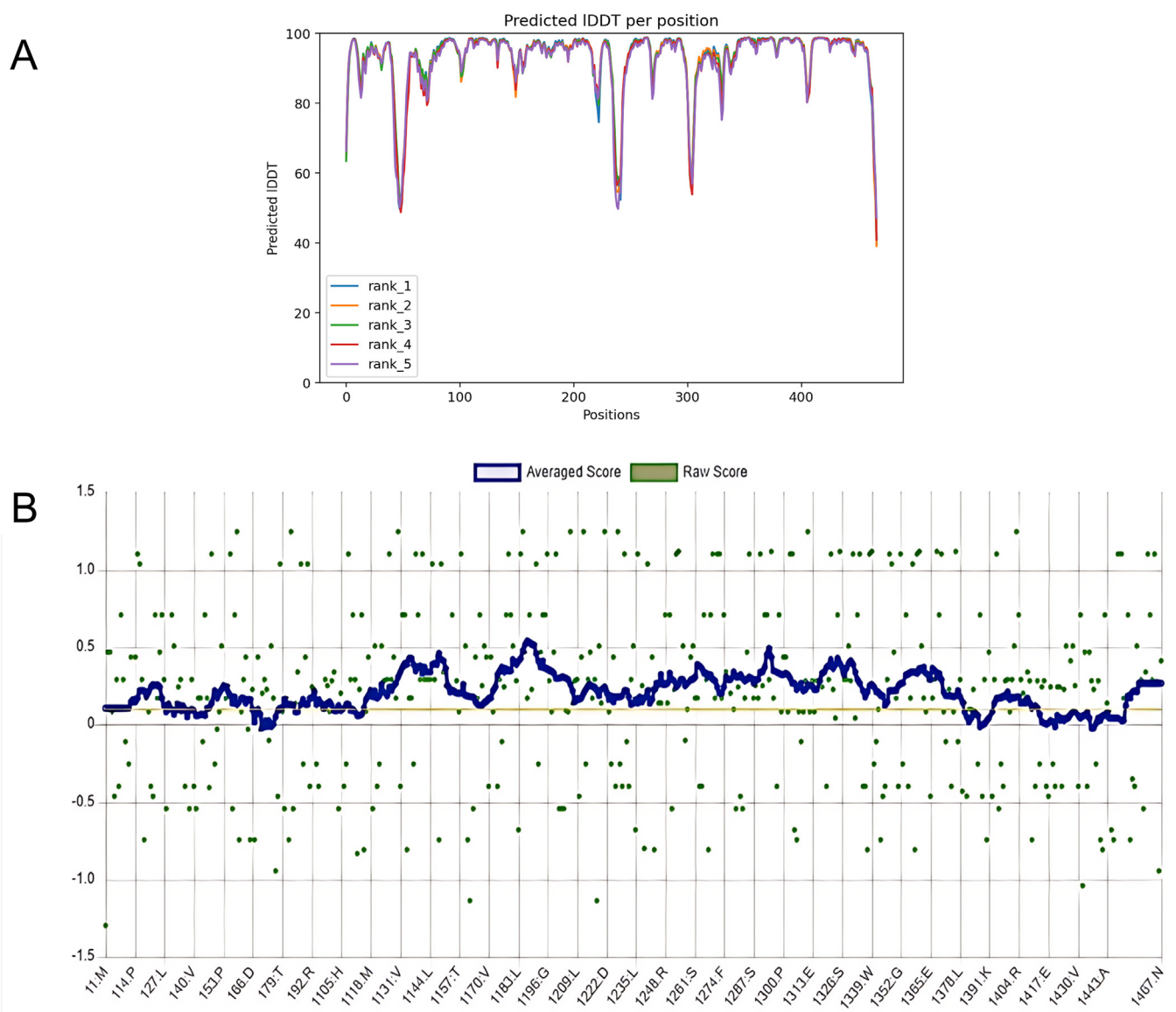


Fig. 5. Quality assessment on structures generated by AlphaFold2. (A) Evaluating AlphaFold predictions. (B) Assessment of model quality of three-dimensional structures by Verify-3D.

In various plant species, including *Arabidopsis*, corn, soybean, and tea, multiple UGTs (UDP-glycosyltransferases) have been extensively studied, highlighting the significance of glycosylation in natural product biosynthesis. In this investigation, a novel glycosyltransferase gene, RpUGT1, was successfully isolated from the medicine herb *R. palmatum*. Through multiple sequence alignment and phylogenetic tree analysis, it was determined that RpUGT1 shares a close phylogenetic relationship with previously reported flavonoid UGTs. The conserved residues within RpUGT1, including the PSPG motif spanning 44 residues, exhibit typical features observed in higher plant glycosyltransferases, further supporting

its classification as a glycosyltransferase (Caputi, Malnoy, Goremykin, Nikiforova, & Martens, 2012; Yin et al., 2017).

It is noteworthy that the UGTs identified in this study, including RpUGT1, exhibit significantly lower catalytic efficiency values (k_{cat}/K_m) towards flavonols compared to previously identified UGTs, such as MeUGT1 and MeUGT2 from *Marchantia emarginata*. Specifically, the k_{cat}/K_m value towards kaempferol for RpUGT1 (10.39 L/mol·S) was 80-fold lower than that for MeUGT1 (820.81 L/mol·S) and about 60-fold lower than that for MeUGT2 (615.08 L/mol·S) (Yuan et al., 2021). To modify the specificity of UGTs, protein structure-guided engineering has emerged as a promising

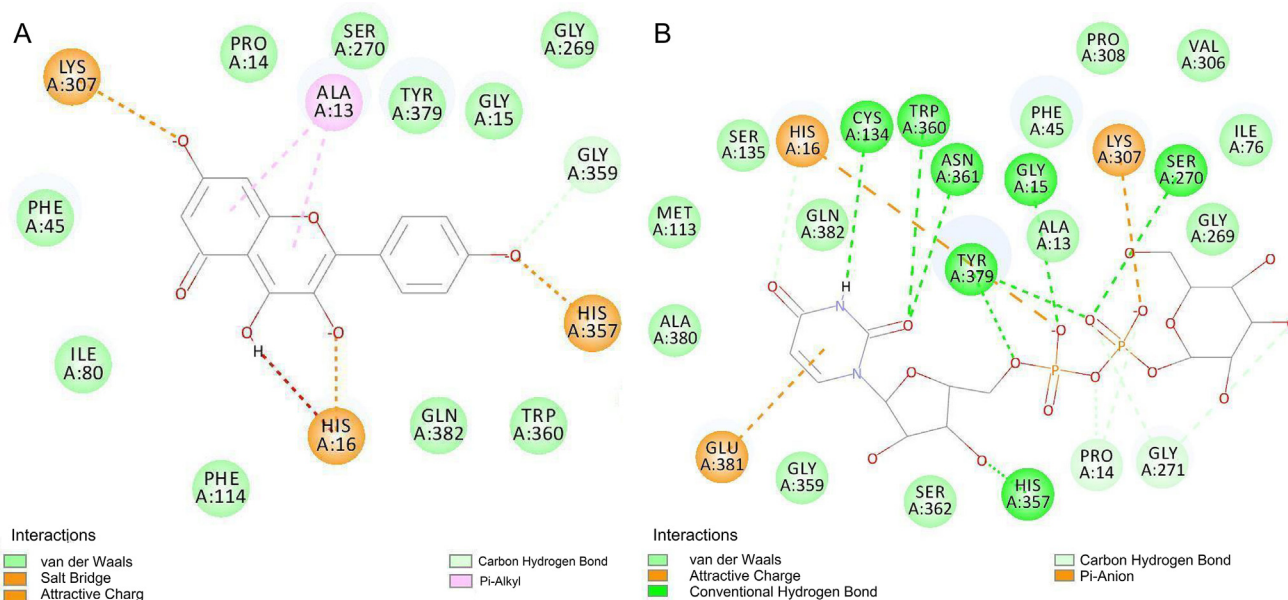


Fig. 6. Auto-Dock analyses of critical residues of RpUGT1. (A) Model of RpUGT1 sugar donor binding pocket. (B) Model of RpUGT1 kaempferol binding pocket shows key residues stabilizing sugar acceptor.

approach, offering opportunities for developing novel and cost-effective production methods using microbes and domesticated plants (Zhang et al., 2019, Vergara, Watson, Watson, Chen, & Lazarus, 2020, Zhang et al., 2020). In the case of RpUGT1, although the key residues have been predicted, further biochemical and structural studies are needed to unveil the detailed reaction mechanism.

5. Conclusion

Moreover, our study successfully cloned and sequenced one UDP-glycosyltransferase gene from *R. palmatum*. The recombinant RpUGT1 enzyme exhibited catalytic activity in the formation of kaempferitrin and isorhamidin from kaempferol and isorhamnetin, respectively. In addition, our homology modeling of RpUGT1 provided valuable insights into its secondary and three-dimensional structure, including identification of catalytic site residues, analysis of hydrogen bond formation, and understanding of substrate binding mechanisms. This investigation has significantly contributed to our understanding of the enzymatic properties of RpUGT1 and has provided experimental evidence supporting the occurrence of glycosylated flavonoid formation *in vivo*.

Credit authorship contribution statement

Shiwen Zhang: Data curation, Project administration, Validation, Writing – original draft. **Jianzhen Zou:** Writing – original draft. **Zitong Hao:** Formal analysis, Visualization. **Mengqi Gao:** Project administration. **Gang Zhang:** Writing – review & editing. **Mengmeng Liu:** Writing – review & editing.

Declaration of competing interest

The authors declare that they have no known competing financial interests or personal relationships that could have appeared to influence the work reported in this paper.

Acknowledgments

This work was financially supported by National Natural Science Foundation (No. 82204567, 8220142901, 82104334), Hebei Natural Science Foundation (No. H2023201005), Shaanxi Provincial Key Industry Innovation Chain (Group) Project (No. 2021ZDLSF04-01), China University Student Innovation and Entrepreneurship Training Program Project (No. 202310075016).

Appendix A. Supplementary material

Supplementary data to this article can be found online at <https://doi.org/10.1016/j.chmed.2024.08.003>.

References

- Akhtar, M. N., Zareen, S., Yeap, S. K., Ho, W. Y., Lo, K. M., Hasan, A., & Alitheen, N. B. (2013). Total synthesis, cytotoxic effects of damnacanthol, nordamnacanthol and related anthraquinone analogues. *Molecules (Basel, Switzerland)*, *18*(8), 10042–10055.
- Cappello, A. R., Dolce, V., Iacopetta, D., Martello, M., Fiorillo, M., Curcio, R., ... Dhanyalayam, D. (2016). Bergamot (*Citrus bergamia* Risso) flavonoids and their potential benefits in human hyperlipidemia and atherosclerosis: An overview. *Mini Reviews in Medicinal Chemistry*, *16*(8), 619–629.
- Caputi, L., Malnoy, M., Goremykin, V., Nikiforova, S., & Martens, S. (2012). A genome-wide phylogenetic reconstruction of family 1 UDP-glycosyltransferases revealed the expansion of the family during the adaptation of plants to life on land. *The Plant Journal: for Cell and Molecular Biology*, *69*(6), 1030–1042.
- Chen, K., Hu, Z. M., Song, W., Wang, Z. L., He, J. B., Shi, X. M., ... Ye, M. (2019). Diversity of *O*-glycosyltransferases contributes to the biosynthesis of flavonoid and triterpenoid glycosides in *Glycyrrhiza uralensis*. *ACS Synthetic Biology*, *8*(8), 1858–1866.
- Dai, X., Zhuang, J., Wu, Y., Wang, P., Zhao, G., Liu, Y., ... Xia, T. (2017). Identification of a flavonoid glucosyltransferase involved in 7-OH site glycosylation in tea plants (*Camellia sinensis*). *Scientific Reports*, *7*(1), 5926.
- Huo, X. W., Zhang, G., & Liu, M. M. (2020). Molecular cloning and enzymatic characteristics of chalcone isomerase from *Rheum palmatum*. *Turkish Journal of Botany*, *44*, 388–395.
- Khan, H., Jawad, M., Kamal, M. A., Baldi, A., Xiao, J., Nabavi, S. M., & Daglia, M. (2018). Evidence and prospective of plant derived flavonoids as antiplatelet agents: Strong candidates to be drugs of future. *Food and Chemical Toxicology: An International Journal Published for the British Industrial Biological Research Association*, *119*, 355–367.
- Koumaglo, K., Gbeassor, M., Nikabu, O., de Souza, C., & Werner, W. (1992). Effects of three compounds extracted from *Morinda lucida* on *Plasmodium falciparum*. *Planta Medica*, *58*(6), 533–534.

- Kumar, M., Singla, R., Dandriyal, J., & Jaitak, V. (2018). Coumarin derivatives as anticancer agents for lung cancer therapy: A review. *Anti-cancer Agents in Medicinal Chemistry*, 18(7), 964–984.
- Kumar, S., Stecher, G., & Tamura, K. (2016). MEGA7: Molecular evolutionary genetics analysis version 7.0 for bigger datasets. *Molecular Biology and Evolution*, 33(7), 1870–1874.
- Li, Y., Baldauf, S., Lim, E. K., & Bowles, D. J. (2001). Phylogenetic analysis of the UDP-glycosyltransferase multigene family of *Arabidopsis thaliana*. *The Journal of Biological Chemistry*, 276(6), 4338–4343.
- Mossa, A. T., Heikal, T. M., Belaiba, M., Raelison, E. G., Ferhout, H., & Bouajila, J. (2015). Antioxidant activity and hepatoprotective potential of *Cedrelopsis grevei* on cypermethrin induced oxidative stress and liver damage in male mice. *BMC Complementary and Alternative Medicine*, 15, 251.
- Mrudulakumari Vasudevan, U., & Lee, E. Y. (2020). Flavonoids, terpenoids, and polyketide antibiotics: Role of glycosylation and biocatalytic tactics in engineering glycosylation. *Biotechnology Advances*, 41, 107550.
- Ono, E., Homma, Y., Horikawa, M., Kunikane-Doi, S., Imai, H., Takahashi, S., ... Nakayama, T. (2010). Functional differentiation of the glycosyltransferases that contribute to the chemical diversity of bioactive flavonol glycosides in grapevines (*Vitis vinifera*). *The Plant Cell*, 22(8), 2856–2871.
- Pei, T., Yan, M., Li, T., Li, X., Yin, Y., Cui, M., ... Zhao, Q. (2022). Characterization of UDP-glycosyltransferase family members reveals how major flavonoid glycoside accumulates in the roots of *Scutellaria baicalensis*. *BMC Genomics*, 23(1), 169.
- Sittie, A. A., Lemmich, E., Olsen, C. E., Hviid, L., Kharazmi, A., Nkrumah, F. K., & Christensen, S. B. (1999). Structure-activity studies: *In vitro* antileishmanial and antimalarial activities of anthraquinones from *Morinda lucida*. *Planta Medica*, 65(3), 259–261.
- Sun, C., Yang, J., Cheng, H. B., Shen, W. X., Jiang, Z. Q., Wu, M. J., ... Wu, M. H. (2019). 2-Hydroxy-3-methylanthraquinone inhibits lung carcinoma cells through modulation of IL-6-induced JAK2/STAT3 pathway. *Phytomedicine*, 61, 152848.
- Vergara, A. G., Watson, C. J. W., Watson, J. M., Chen, G., & Lazarus, P. (2020). Altered metabolism of polycyclic aromatic hydrocarbons by UDP-Glycosyltransferase 3A2 missense variants. *Chemical Research in Toxicology*, 33(11), 2854–2862.
- Wang, M., Dong, B., Song, Z., Qi, M., Chen, T., Du, T., ... Fu, U. (2023). Molecular mechanism of naringenin regulation on flavonoid biosynthesis to improve the salt tolerance in pigeon pea (*Cajanus cajan* (Linn.) Millsp.). *Plant Physiology and Biochemistry*, 196, 381–392.
- Xie, L., Cao, Y., Zhao, Z., Ren, C., Xing, M., Wu, B., ... Li, X. (2020). Involvement of *MdUGT75B1* and *MdUGT71B1* in flavonol galactoside/glucoside biosynthesis in apple fruit. *Food Chemistry*, 312, 126124.
- Xu, J., Liao, B., Yuan, L., Shen, X., Liao, X., Wang, J., ... Chen, S. (2022). 50th anniversary of artemisinin: From the discovery to allele-aware genome assembly of *Artemisia annua*. *Molecular Plant*, 15(8), 1243–1246.
- Xu, Z., Chen, Q., Zhang, Y., ... Liang, C. (2021). Coumarin-based derivatives with potential anti-HIV activity. *Fitoterapia*, 150, 104863.
- Yin, Q., Shen, G., Di, S., Fan, C., Chang, Z., & Pang, Y. (2017). Genome-wide identification and functional characterization of UDP-glucosyltransferase genes involved in flavonoid biosynthesis in glycine max. *Plant & Cell Physiology*, 58(9), 1558–1572.
- Yuan, J. C., Xiong, R. L., Zhu, T. T., Ni, R., Fu, J., Lou, H. X., & Cheng, A. X. (2021). Cloning and functional characterization of three flavonoid O-glucosyltransferase genes from the liverworts *Marchantia emarginata* and *Marchantia paleacea*. *Plant physiology and Biochemistry*, 166, 495–504.
- Zhai, Y., Zhang, T., Guo, Y., Gao, C., Zhou, L., Feng, L., ... Xumei, W. (2023). Phylogenomics, phylogeography and germplasm authentication of the *Rheum palmatum* complex based on complete chloroplast genomes. *Journal of Plant Research*, 136(3), 291–304.
- Zhang, M., Li, F. D., Li, K., Wang, Z. L., Wang, Y. X., He, J. B., ... Ye, M. (2020). Functional characterization and structural basis of an efficient di-C-glycosyltransferase from *Glycyrrhiza glabra*. *Journal of the American Chemical Society*, 142(7), 3506–3512.
- Zhang, Z., Li, R., Aweya, J. J., Wang, F., Zhong, M., & Zhang, Y. (2019). Identification and characterization of glycosylation sites on *Litopenaeus vannamei* hemocyanin. *FEBS Letters*, 593(8), 820–830.